Fermi National Accelerator Laboratory

FERMILAB-CONF-88/156-T
October, 1988

WEAK DECAY AMPLITUDES IN LARGE N_C QCD

William A. Bardeen

Theoretical Physics Department
Fermi National Accelerator Laboratory
P.O. Box 500, Batavia, IL 60510

Talk presented at the Workshop on
Hadronic Matrix Elements and Weak Decays
Ringberg Castle, Bavaria
April 17-23, 1988

ABSTRACT

A systematic analysis of nonleptonic decay amplitudes is presented using the large N_C expansion of quantum chromodynamics. In the K-meson system, this analysis is applied to the calculation of the weak decay amplitudes, weak mixing and CP violation.

Operated by Universities Research Association Inc. under contract with the United States Department of Energy

1. INTRODUCTION

Precision tests of the standard model of the electroweak interactions are an essential component in establishing the validity of the specific model or the directions for new physical processes. Many tests require knowledge of the strong interaction component of the model. The short distance contributions have been previously understood in terms of perturbative QCD. The large distance effects are not described by the perturbative picture, and various estimates of these contributions have been made previously. In most cases, the approximate methods for treating the long distance contributions, such as factorization, have been inconsistent with the short distance analysis given by perturbative QCD. In this talk, I will present a consistent analysis of both the short and long distance components using the large N_C expansion method to analyse the strong interaction effects[1].

In Section 2, I briefly describe the large N_C expansion method and then apply it to the standard analysis of the short distance perturbative contributions in Section 3. An alternative, bosonized version of QCD is described in Section 4 and used to obtain the consistent formulation of the theory presented in Section 5. The method is then applied to the weak decay amplitudes for $K\to\pi\pi$, for the B_K parameter of $K^0\rightleftarrows\overline{K^0}$ mixing and for the ε'/ε parameter of direct CP violation.

2. QCD IN THE LARGE N_C LIMIT

The large N_C limit of quantum chromodynamics has received much attention in the past[2]. In this limit, the number of colors, N_C, is large but the gauge coupling constant goes to zero such that the combination, $\underline{\alpha} = \alpha_C \cdot N_C$, is held fixed. At leading order in the large N_C expansion, the theory greatly simplifies and the higher order terms can be systematically calculated. This method was applied to a number of models in two dimensions where exact solutions could be obtained[3]. The structure of the large N_C limit can be most clearly seen from an analysis of the Feynman diagrams.

2.1. Diagram Analysis

At large N_C, the color structure of the Feynman diagrams for any process can be analysed by observing that the gluon propagator can be viewed as having quark-antiquark color indices and the quark color lines determine the appropriate color factors. For a gluon exchange diagram

for quark-antiquark scattering ($\overline{1}+3 \rightarrow \overline{2}+4$), the color factors are

$$(\lambda^a/2)_{12} \cdot (\lambda^a/2)_{43} = (1/2)\, \delta_{13}\delta_{42} - (1/2N_C)\, \delta_{12}\delta_{43} \qquad (1)$$

where $\{\lambda^a\}$ are the color coupling matrices. At large N_C, the second term is suppressed and the color couplings are simplified.

The leading diagrams have a planar gluon structure. Adding additional gluons which preserve the planar structure are higher order in the fixed coupling, $\underline{\alpha}$, but do not change the order of the large N_C expansion. Hence, each order of the large N_C expansion will involve an infinite class of Feynman diagrams to all orders in $\underline{\alpha}$.

The insertion of internal fermion loops will add extra powers of the gauge coupling constant without extra color factors and are generally suppressed by a factor of $1/N_C$ for each additional internal quark loop. Diagrams with nonplanar gluon interactions are suppressed by factors of $(1/N_C)^2$.

The large N_C expansion produces a kind of interacting string theory. The planar diagrams have the structure of a propagating world sheet where the string coupling constant is $O(1/N_C)$. Quark loops are associated holes or boundaries on the world sheet. The nonplanar diagrams have the structure of higher genus surfaces. It is intriguing to speculate on the connection between the large N_C expansion of QCD and a dynamical string picture for hadrons.

2.2 Strong Dynamics

While the large N_C expansion greatly simplifies the structure of the Feynman diagrams, it is still a complex dynamical theory in four dimensions. I will briefly review the basic features of the leading order theory.

2.2.1. The effective coupling constant, $\underline{\alpha}$, runs as in regular QCD due to the presence of gluon loops although the fermion loop contributions are suppressed. The short distance perturbative β-function given by, $\beta(\underline{\alpha}) = -(11/6\pi) \cdot \underline{\alpha}^2$. The short distance theory is asymptotically free and the perturbative picture should apply.

2.2.2. The attractive gauge interactions should stimulate a dynamical breaking of chiral symmetry. Nontrivial chiral condensates will exist, $\langle \overline{\Psi}\Psi \rangle_0 \neq 0$, and the boundstate spectrum will include the usual Goldstone bosons, $\pi, K, \eta, \cdots$.

2.2.3. From the structure of the perturbative β-function, we also expect the theory to have confinement at large distance. Gluon condensates will play the same role as in regular QCD. However, the effects of small instantons are suppressed being of order, $\exp(-1/\alpha) \approx \exp(-N_C)$. Of course, it is not clear whether a dilute gas of small instantons has any affect on the confinement mechanism. The large scale color fluctuations which are responsible for confinement may remain unsuppressed. We will assume, not prove, that the large N_C theory is confining and produces the usual spectrum of hadronic boundstates.

2.2.4. The spectrum of the large N_C theory should consist of quark-antiquark boundstates which form infinite trajectories of narrow resonances. The lowest mass states will be the usual pseudoscalar mesons which are massless in the chiral limit. Note that effects related to the axial vector anomalies are suppressed contrary to QCD where the anomaly produces an explicit chiral U(1) breaking. There should also exist trajectories of narrow resonances for the glueball states.

2.2.5. The resonances are narrow as the decay amplitudes are suppressed in the formal large N_C limit. The diagrams describing the interactions of the normal meson boundstates will include factors of $1/\sqrt{N_C}$ for each external meson in addition to the normal large N_C color factors. Hence, a two body meson decay amplitude is $O(1/\sqrt{N_C})$ and a two meson scattering amplitude is $O(1/N_C)$. At leading N_C, the planar quark-gluon diagrams can only produce tree diagrams for the meson scattering amplitudes as there are no internal quark loops to generate the multimeson intermediate states. Again this structure is similar to the string theory amplitudes. The amplitudes of the large N_C theory may not have the same duality properties as the fundamental string amplitudes.

2.3 Operators

Local quark operators for currents and densities will have nontrivial meson matrix elements. The meson decay constants arise from a direct coupling of the currents to the appropriate mesons. The color structure implies that the meson decay constants are $O(\sqrt{N_C})$, $F_\pi \approx N_C \cdot (1/\sqrt{N_C}) \approx \sqrt{N_C}$, etc. There will also be form factors for the various meson matrix elements. Since the leading N_C amplitudes

correspond to meson tree amplitudes, there should exist a local meson representation of the color singlet quark currents and quark densities.

2.4. Meson Loop Expansion

The strong interaction dynamics produces meson tree amplitudes at leading order in the large N_C expansion. Unitarity will demand that meson loop contributions must be included in a complete treatment of the theory. Meson loop contributions come higher orders in the large N_C expansion. Indeed, the insertion of an internal quark loop will generate a meson loop contribution which is suppressed by a factor of $1/N_C$. A two meson loop contribution can only arise from diagrams containing two internal quark loops or nonplanar gluon contributions which are $O(1/N^2_C)$. I note that the only ultraviolet divergences specific to the meson loop diagrams are those divergences already contained in perturbative QCD.

3. WEAK DECAY AMPLITUDES

In the standard model, the basic $\Delta S=1$ weak transitions are given by an effective current-current interaction generated by a W-boson exchange,

$$H_{Wk} = -(G_F/\sqrt{2})\cdot s_1\cdot c_1\cdot c_3 \cdot(\overline{S}\,U)_L \cdot D_W(Q^2) \cdot(\overline{U}\,D)_L \qquad (2)$$

where (s_1,c_1,c_3) are determined by the KM angles and $D_W(Q^2)$ is the W-boson propagator. Using the large N_C expansion, the various contributions to the weak decay amplitudes can be determined.

3.1. Leading Order Diagrams

At leading N_C, the strong dynamics affects each current separately, as shown in Figure 1a. Hence the meson matrix elements obey the factorization rule[4] where the hadronization of each current is independent of the other. These current matrix elements contain only planar diagrams and are, therefore, given by the meson tree amplitudes.

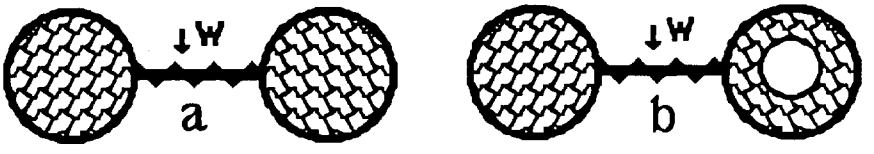

Figure 1: Factorized Amplitudes

3.2. Next Order Factorized Diagrams

To next order in the large N_C expansion, there are factorized contributions coming from the meson loop amplitudes which arise from inserting an internal quark loop on one side of the W-boson interaction as shown in Figure 1b. When these contributions are combined with the previous leading order contributions, the full factorized amplitude is obtained. However, the Fierz contributions which are usually part of the factorized amplitudes are not included here but are part of the nonfactorized amplitudes considered next.

Figure 2: Nonfactorized Amplitudes

3.3. Next Order Nonfactorized Diagrams

The remaining contributions to this order in the large N_C expansion are contained in the diagrams of Figure 2. Actually all diagrams shown here have the same structure and differ only in the location of the external meson states. These diagrams contain all the short distance physics associated with the quark evolution, weak mixing and penguin contributions. They also are responsible for all of the nonfactorizing strong interaction corrections to the weak matrix elements.

3.4. Weak Evolution at Large N_C

The usual treatment of weak matrix elements involves the separation of the short and long distance contributions using an intermediate normalization scale. For low energy matrix elements, the full weak Hamiltonian can be replaced by an effective Hamiltonian[5]

$$H_{wk} \rightarrow H_{eff} = -(G_F/\sqrt{2})\cdot s_1\cdot c_1\cdot c_3 \cdot \sum_i \tilde{R}_i(\mu)\cdot Q_i(\mu) \qquad (3)$$

where the short distance physics is contained in the coefficient functions, $\tilde{R}_i(\mu)$, and the long distance physics is contained in the matrix elements of the induced weak operators, $Q_i(\mu)$. In the standard model, the coefficient functions can be further separated by their dependence

on the KM parameters,

$$\tilde{R}_i(\mu) = \tilde{z}_i(\mu) + \tau \cdot \tilde{y}_i(\mu), \quad \tau = s_2 \cdot s_2 + (s_2 \cdot s_3 \cdot c_2 / c_1 \cdot c_3) \cdot e^{-i\delta} \qquad (4)$$

If the strong interactions are ignored, the effective Hamiltonian of Eq.(3) reduces to that of Eq.(2). In the usual treatment[5], various four fermion operators are generated including current-current operators and those associated with penguins.

Because they are only sensitive to the short distance physics, the coefficient functions can be computed using perturbative QCD and the appropriate renormalization group equations. The solution is expressed in terms of the anomalous dimension matrix, $\{\gamma(\alpha(Q^2))\}_{ij}$, describing the evolution of the weak operators.

$$\tilde{z}(\mu)_{ij} = \{\exp(-\int_{\mu^2}^{m^2} (dQ^2/2Q^2) \cdot \gamma(\alpha(Q^2))\}_{ij} \qquad (5)$$

The anomalous dimension matrix can be computed directly from the perturbative quark-gluon diagrams. From the structure of these diagrams, all relevant terms in the anomalous dimension matrix are $O(1/N_C)$[1].

The full matrix elements of the effective weak Hamiltonian, Eq.(3), can be decomposed according to the large N_C expansion.

$$\langle O_i(m^2)\rangle_{full} = \langle Q_i(\mu)\rangle_{LO} + \langle Q_i(\mu)\rangle_{F(1/N)} \qquad (6)$$

$$+ \langle Q_i(\mu)\rangle_{NF(1/N)} - \int_{\mu^2}^{m^2} (dQ^2/2Q^2) \cdot \{\gamma(\alpha(Q^2))\}_{ij} \cdot \langle Q_j(\mu)\rangle_{LO}$$

$$+ \text{higher order terms}$$

The leading order matrix element, $\langle Q_i(\mu)\rangle_{LO}$, corresponds to Figure 1a and the (1/N) factorized matrix element, $\langle Q_i(\mu)\rangle_{F(1/N)}$, corresponds to Figure 1b. The diagrams of Figure 2 correspond to sum of the nonfactorizing part of the weak matrix element, $\langle Q_i(\mu)\rangle_{NF(1/N)}$, and the part due to the anomalous dimension evolution. For a consistent treatment of the weak matrix elements, the nonfactorizing part of the weak matrix element must be computed to the same order as the weak evolution as they are both a part of a single term in the large N_C

expansion. Only a consistent calculation can be expected to be independent of the normalization scale, μ.

4. BOSONIZATION

4.1. Dual Meson Theory

At the fundamental level, QCD is formulated as a theory of quarks and gluons. The large N_C expansion implies the existence of an equivalent, dual meson representation of QCD. As noted in Section 2, the leading N_C theory consists of infinite trajectories of stable meson resonances.

The strong interactions of these mesons can be deduced from the leading $1/N_C$ corrections. The leading order terms produce meson tree amplitudes from which an effective meson Lagrangian can be derived. This theory involves the infinite towers of resonances and the correct implementation of an effective Lagrangian formalism will confront questions related to the precise duality properties of the scattering amplitudes, similar to the problem that confronted the proper formulation of string field theory. In addition to the strong interaction dynamics, there will be a local meson representation of all color singlet operators including the weak currents and quark densities. Of course, the structure of these operators is closely related to the effective meson Lagrangian describing the strong interaction dynamics.

The large N_C expansion produces an effective theory that seems closely related to the string theories. Indeed, string theory was originally derived from the phenomenological structure of hadronic physics. The original attempts to apply a fundamental string picture to hadrons failed to produce a consistent theory. However, the hadronic string picture may differ from the fundamental string picture in a number of ways. Hadronic strings may have a finite size or a more complicated action which is not contained within the scope of conformal field theories. Perhaps a more crucial difference concerns the known existence of valence quark and gluon structure. This pointlike structure is responsible for all of the hard processes in QCD, such as jets and scaling, but is absent in the fundamental string picture.

Some hint for the existence of an hadronic string picture is provided by the Lovelace-Veneziano formula[6] for π-π scattering. This scattering amplitude is a tree meson amplitude involving an infinite tower of mesons which has the proper high energy behavior as well as

the low energy theorems of chiral current algebra.

$$A_{1234} = tr\{\tau^1\tau^2\tau^3\tau^4\}\cdot(8\cdot\pi\cdot\alpha'\cdot f^2_\pi)^{-1}\cdot\Gamma(1-\alpha(s))\Gamma(1-\alpha(t))/\Gamma(1-\alpha(s)-\alpha(t)) \qquad (7)$$

$$+ \text{ permutations,}$$

where $\alpha(s) = 1/2 + \alpha'\cdot s$ is the usual ρ-meson, Regge trajectory. This amplitude is probably the exact leading N_C scattering amplitude for π-π scattering. Unfortunately, we do not yet know the other strong interaction amplitudes or any of the amplitudes involving quark currents or densities.

4.2. Truncation of the Meson Theory

The complete meson theory may not be required to study the low energy behavior of meson amplitudes. The low energy theory is sensitive only to the low mass states and their interactions. However, we can not simply ignore the heavy states but must make a proper low energy truncation of the full meson theory. As a first approximation, it may be possible to use a nonlinear σ model including loop effects for the low energy dynamics of the Goldstone bosons, π, K, η ···.

An example of the decoupling of the heavy states is given by the linear σ model. In this model the π-π scattering amplitude is given by ($m^2_\sigma = m^2$)

$$A_{1234} = \delta_{12}\delta_{34}\cdot\lambda\cdot[\ 1 + m^2/(q^2-m^2)\ ] \qquad (8a)$$

$$= \delta_{12}\delta_{34}\cdot\lambda\cdot[\ -q^2/m^2 + (q^2)^2/m^2(q^2-m^2)\ ] \qquad (8b)$$

If we simply ignored the contribution of the heavy states, we would be forced to drop the σ exchange term in Eq.(8a). The resulting amplitude would not have the correct low energy behavior which is given by the first term in Eq.(8b) and corresponds to amplitude of a nonlinear σ model. From Figure 3, we see that the nonlinear σ model is only a good approximation at low energy and it makes no sense to interpret its high energy behavior as it vastly differs from the behavior of the full amplitude. If we are to truncate the full theory to the nonlinear σ model, then it is essential to introduce a physical cutoff to define the

range of momenta where the nonlinear model represents a good approximation. Of course, in our case the full amplitude is not given by the linear σ model but by quantum chromodynamics, with an amplitude more closely related to the string amplitude given in Eq.(7).

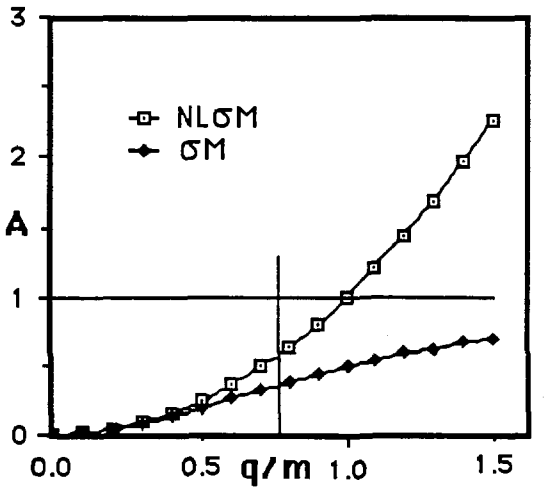

Figure 3: σ Model decoupling

The effective low energy theory will be correctly described by a nonlinear σ model only in the low energy limit. The truncation of the full amplitudes will generate corrections terms which can be viewed as higher derivative interactions, etc. As the amplitudes are extrapolated to higher momentum scales, some of the heavy states will have to be included in the explicit dynamics of the truncated theory.

4.3. Chiral Lagrangians

The lowest energy truncation of QCD which describes the interactions of the chiral Goldstone bosons is given by the effective chiral Lagrangian,

$$L = (1/4)\cdot f^2_\pi \cdot\{\, tr[\, D^\mu U \cdot D_\mu U^+ \,] + r\cdot tr[\, m^+\cdot U + U^+\cdot m \,]\,\}$$

$$+ (1/4)\cdot f^2_\pi \cdot(r/\Lambda^2_\chi)\cdot tr[\, m^+\cdot D^2 U + D^2 U^+\cdot m \,] + \cdots\cdots \qquad (9)$$

where $U = U(\pi)$ is the chiral matrix and $D^\mu = \partial^\mu + i\cdot W^\mu x$ is a covariant derivative used to consistently generate the current interactions. The first line of Eq.(9) gives the unique, lowest order terms in the effective action where f_π and r are dynamical parameters and m is the quark

mass matrix. We have also included one higher derivative interaction as it is required to generate the penguin operator matrix elements; there are certainly many other terms which could be included[7]. This Lagrangian ignores anomalies and the U(1) problem which play no direct role in the weak decay amplitudes studied in this paper; we will assume that there is a large singlet mass term for the singlet η' meson reflecting the strong anomalies and consistent with phenomenology.

The meson representation of the weak currents is obtained directly from the Lagrangian of Eq.(9),

$$(\overline{\Psi}^j \gamma_\mu \Psi_i)_L = i\,(f^2_\pi/2)\cdot\{\,[\,(\partial_\mu U)\cdot U^+ - U\cdot(\partial_\mu U^+)\,] - (r/\Lambda^2_\chi)\cdot[\,m\cdot(\partial_\mu U^+) - (\partial_\mu U)\cdot m^+\,] + \cdots\cdots\,\}_{ij} \qquad (10)$$

Similar expression are obtained for the quark densities

$$(\overline{\Psi}^j{}_R\, \Psi_{Li}) = -\,(f^2_\pi/4)\cdot r\cdot\{\,U - (1/\Lambda^2_\chi)\cdot\partial^2 U + \cdots\cdots\,\}_{ij} \qquad (11)$$

where again we include terms which are contained in the leading N_C expansion but are higher order in the derivative expansion for the low energy amplitude.

4.4. Renormalization

As noted in Section 2, the $1/N_C$ expansion is a loop expansion in the full meson theory. The leading N_C contributions are provided by evaluating the the expressions given in the previous section in tree approximation. In the full meson theory, the next corrections are obtained by evaluating the one loop diagrams of the full meson theory. The low mass, low momentum contributions generate the correct infrared structure which is required to maintain the proper unitarity relations at low energy. These contributions are correctly given by the loop corrections to the chiral Lagrangian[6]. The high mass or high momentum loops of the full meson theory are not those of the chiral Lagrangian but reflect the complete structure of QCD. They will generate effective counterterms for the truncated chiral Lagrangian theory which are insensitive to the infrared behavior of the theory.

We can use the chiral Lagrangian to compute the low energy contributions so long as we introduce a physical momentum cutoff to

preserve the validity of the truncation. A background field calculation[1] shows that the leading contributions come from terms which have a quadratic dependence on the cutoff scale and these serve only to renormalize the effective value of the Lagrangian value of the parameter, f_π.

To determine the lagrangian parameters, we calculate the physical decay constants, F_K and F_π, including the effects of the chiral breaking terms and obtain the relations

$$F_K/F_\pi = 1 + (m^2_K - m^2_\pi)/\Lambda^2_\chi - (1/8f^2_\pi)\cdot[\, 2\cdot I_2(m^2_K) - 5\cdot I_2(m^2_\pi) + 3\cdot I_2(m^2_8)\,] \tag{12}$$

where $I_2(m^2) = (4\pi)^{-2}\cdot[\, M^2 - m^2\cdot\log(1+M^2/m^2)\,]$ and

$$f^2_\pi(M^2) = F^2_\pi + 2\cdot I_2(m^2_K) + I_2(m^2_K) = M^2/(4\pi)^2 + O(1/N_C) \tag{13}$$

Using this parameterization, the $1/N_C$ corrections to F_K/F_π are at most 6% for any reasonable value of the physical cutoff.

The value of Λ_χ is found to be 1000 MeV compared to the value of 900 MeV found by a leading order analysis. The value of this parameter is important as it determines the size of the penguin matrix elements. The meson representation of the penguin operator is given by

$$Q_6 = -8\cdot\{\, \sum_q (\bar{S}_L\, q_R)\cdot(\bar{q}_R\, D_L)\,\} \rightarrow 4\cdot f^2_\pi\cdot(r/\Lambda^2_\chi)\cdot\{\, \partial\mu U\, \partial_\mu U^+\,\}_{ds} \tag{14}$$

where we note that the only these tree amplitudes are required to specify the penguin matrix elements to leading order in the large N_C expansion.

5. CONSISTENT WEAK DECAY AMPLITUDES

The large N_C expansion provides a framework for a systematic and consistent evaluation of the weak decay amplitudes. By analysing the

strict large N_C expansion, a consistent estimate of the weak matrix elements can be achieved and combined with the usual perturbative renormalization group analysis of the short distance physics.

5.1. Factorized Amplitudes

For the leading order terms, the diagrams of Figure 1a contribute. Since all components of the matrix elements are at low energy, the meson representation of the weak currents can be used directly to calculate the tree matrix elements. The amplitude is necessarily factorized as the hadronization of each current is independent of the other. This approximation corresponds to the usual vacuum insertion calculation where the Fierz rearrangement terms are not included.

The meson loop corrections of Figure 1b generate the strong interaction corrections to the matrix elements of the weak currents. These contributions include the explicit loop corrections of the truncated theory and the appropriate counter terms[8] which reflect our inability to compute the short distance components of the loops of the fully bosonized meson theory. These diagrams obey the same factorization properties as the leading terms. Indeed, the full factorized amplitude, to this order, is given by the sum of these corrections with the leading order terms. The explicit loops of the truncated theory generate the nonanalytic dependence and sensitivity to the meson masses and momenta. In principle, the factorized contributions can be determined directly from experiment by measuring the purely semileptonic processes to obtain the appropriate meson current matrix elements. It is only the nonfactorized amplitudes which remain to be determined from the explicit calculation.

5.2. Nonfactorized Amplitudes

The class of diagrams shown in Figure 2 are responsible for the nonfactorized components of the weak matrix elements to this order in the large N_C expansion. All other terms are higher order in $1/N_C$. The two currents are fully connected by the strong interactions. However, this amplitude has an extremely simple structure in the large N_C limit which we can exploit for a complete calculation of both the short and long distance contributions. The amplitude can be represented by a convolution of the W-boson propagator with a meson tree amplitude,

$$A(p_1, \cdots, p_n) = i\cdot(2\pi)^{-4}\cdot\int dq\, D^{\mu\nu}{}_W(q)\cdot A_{\mu\nu}(q,p_1, \cdots, p_n) \qquad (15)$$

As noted in Section 3, this amplitude is responsible for all of the usual weak evolution (quark evolution, penguins, etc) as well as the nonfactorizing long distance corrections to the weak matrix elements. The amplitude appearing in the integrand of Eq.(15) is a meson tree amplitude with external currents.

The short and long distance contributions are controlled by the explicit momentum flowing through the W-boson propagator. These contributions can be separated, at least in principle, by a suitable regularization of this integration. An explicit example is provided by the analytic regularization

$$D^{\mu\nu}{}_W(q) \to D^{\mu\nu}{}_W(q)\cdot\{\,[\,q^2/(q^2-M^2)\,] + [\,-M^2/(q^2-M^2)\,]\,\} \qquad (16)$$

The first term above contributes at short distance but is suppressed at low momentum. The second term contributes at long distance but the high momentum components are suppressed. This separation can be exploited to use the quark-gluon representation to calculate the first term and a truncated meson Lagrangian for the second term. It should be noted that the only ultraviolet divergences associated with the momentum integration are those of perturbative QCD which are contained within the quark-gluon analysis. The analytic reqularization used in Eq.(16) may be too smooth for realistic calculations where the truncated meson theory diverges rapidly from the correct physics beyond the cutoff scale.

5.3. Short Distance Contributions (Quark Picture)

If the cutoff scale, M^2, is taken sufficiently large, then only the high momentum part of the integration will contribute to the amplitude in Eq.(15) and perturbative QCD can be used for the calculation. For a regularization such as given in Eq.(16), we can simply use the expansion in Eq.(6) to compute the contribution from the cutoff M^2 to m^2_W. The matrix element will be given by

$$\langle O_i(m^2)\rangle_{\text{regulated}} \approx \langle O_i(m^2)\rangle_{\text{full}} - \langle O_i(M^2)\rangle_{\text{full}}$$

$$= \{\,-\int_{\mu^2}^{m^2} (dQ^2/2Q^2)\cdot\{\gamma(\alpha(Q^2))\}_{ij}\cdot\langle Q_j(\mu)\rangle_{LO}\,\}$$

$$- \{ -\int_{\mu^2}^{M^2} (dQ^2/2Q^2) \cdot \{\gamma(\alpha(Q^2))\}_{ij} \cdot \langle Q_j(\mu)\rangle_{LO} \} \qquad (17)$$

$$= -\int_{M^2}^{m^2} (dQ^2/2Q^2) \cdot \{\gamma(\alpha(Q^2))\}_{ij} \cdot \langle Q_j(\mu)\rangle_{LO}$$

which is just the normal weak evolution to the infrared regulator scale, M^2.

This contribution can also be computed directly from the perturbative diagrams. If the momentum of the W-boson propagator is taken to be large in Figure 4a, then the leading short distance contribution comes from the box diagram contribution where the gluon has been expanded out of the the hadronic matrix element using the operator product expansion as in Figure 4b. The diagram of Figure 4c has a high momentum contribution from the explicit box diagram as shown in Figure 4d. High momentum contributions from wavefunction gluons will be higher order in perturbative QCD.

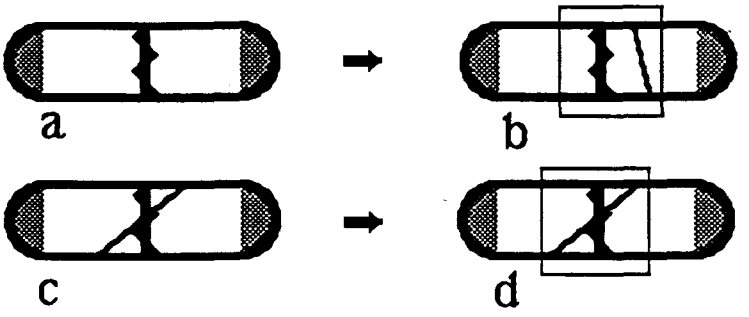

Figure 4: Direct Calculations

These short distance diagrams are just the usual weak mixing diagrams used to calculate the anomalous dimensions of Eq.(6) where M^2 replaces the infrared normalization scale, μ^2. This gives precisely the same result as Eq.(17) except for finite corrections related to the normalization prescription dependence of the subtraction procedure which can be modified to agree with the explicit diagram calculation. Using the result in Eq.(17), the scale dependence of the regulated matrix element is given by

$$M^2\partial_{M^2} \langle O_i(m^2)\rangle_{regulated} = (1/2) \cdot \{\gamma(\alpha(M^2))\}_{ij} \cdot \langle Q_j(\mu)\rangle_{LO} \qquad (18)$$

where the leading order matrix element, $\langle Q_j(\mu)\rangle_{LO}$, is actually

independent of the normalization scale, μ.

5.4. Fierz Terms

The above result depends on the the structure of the external states. It was essential that the meson matrix elements produced no hard momentum components except for those generated by perturbative QCD.

Hence the diagrams of Figure 4a do not yield any direct Fierz contributions for the high momentum components. However, the Fierz contributions will be generated if the external have explicit hard components, such as pointlike couplings to external particles (Higgs, axions, etc) or heavy quark systems (quarkonia, etc). When they can contribute, the direct Fierz terms are opposite in sign to the terms generate by the normal weak evolution. This may have some relation to the suppression of the $1/N_C$ corrections for D-meson decays, etc.

5.5. Long distance Contributions (Meson Picture)

The long distance contributions come from the low momentum part of the integral of Eq.(15). For low momentum external meson states, the meson amplitude in the integrand is completely determined by the low energy effective theory. The truncated chiral Lagrangian given in Eq.(9) represents the simplest, first approximation to the integrand amplitude.

Using this chiral Lagrangian, the leading contributions from the loop integration are the quadratic divergences. In the chiral limit, the integrals can be done for arbitrary, low momentum meson states. Using a coset representation of the chiral fields, the resulting matrix elements are given by

$$\langle Q_1(M^2)\rangle = -\,2\cdot M^2\cdot(4\pi\cdot f^2_\pi)^{-2}\cdot\langle Q_2(0)\rangle_{LO} \tag{19}$$

$$\begin{aligned}\langle Q_2(M^2)\rangle &= -\,2\cdot M^2\cdot(4\pi\cdot f^2_\pi)^{-2}\cdot\langle Q_1(0)\rangle_{LO} \\ &\quad + M^2\cdot(4\pi\cdot f^2_\pi)^{-2}\cdot\langle Q_2(0)-Q_1(0)\rangle_{LO} \qquad (20)\\ &= -\,2\cdot M^2\cdot(4\pi\cdot f^2_\pi)^{-2}\cdot\langle Q_1(0)\rangle_{LO} \\ &\quad + (\Lambda^2_\chi/4\cdot r^2)\cdot M^2\cdot(4\pi\cdot f^2_\pi)^{-2}\cdot\langle Q_6(0)\rangle_{LO} \qquad (21)\end{aligned}$$

where the explicit forms of the leading order matrix elements have been

used to introduce the penguin operator. With this identification, the mixing structure of the operator matrix elements agrees precisely with the weak mixing computed from the quark diagrams. We can use the above result to compute a meson anomalous dimension matrix.

$$M^2\partial_{M^2}\langle Q_i(M^2)\rangle = -(1/2)\cdot\{\gamma_{meson}(M^2)\}_{ij}\cdot\langle Q_j(0)\rangle_{LO} \qquad (22)$$

If the quark-gluon amplitudes and the meson amplitudes were both exact then the quark-gluon and meson anomalous dimensions would be identical so that the sum of the quark and meson amplitudes would be independent of the matching scale, M^2, see Eqs.(18,22). However, we have used extreme truncations for both theories, leading logs for the quark-gluon theory and the simplest chiral Lagrangian for the meson theory. At best, we would only expect these calculations to agree in an overlap region where both theories are valid approximations. In Figure 5, the two anomalous dimensions are shown as a function of the regulator scale, M, and are seen to agree for scales around 600 MeV. This seems to be a reasonable matching scale as meson amplitudes should begin to feel the suppression effects of the vector meson form factors while still above the constituent mass scale of the quarks. The severe truncations of both the quark-gluon and meson calculations do not permit the existence of a large crossover region. However, it is the fact that these two calculations yield similar results which is responsible for the consistency of the result.

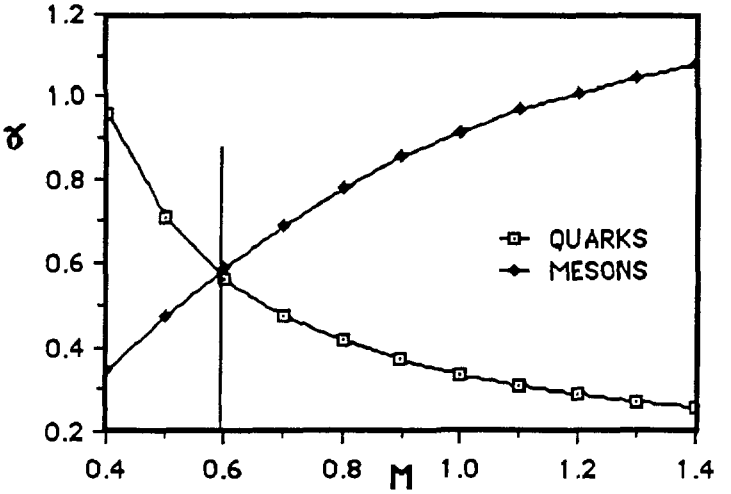

Figure 5: Anomalous Dimensions vs matching scale (GeV)

Clearly, there is much room for improvement of these calculations. The quark theory could be extended to higher order in perturbative QCD, and the effects of dynamical symmetry breaking could be included. The meson theory could be improved by including higher derivative terms and/or meson resonances such as ρ, K^*, A_1, etc.

6. Applications

6.1. $K \to \pi\pi$ Decay Amplitudes

The K-meson decay amplitudes have long been a puzzle due to the large enhancement (suppression) of the $\Delta I=1/2$ ($\Delta I=3/2$) amplitudes. The normal short distance evolution and the penguin contributions explain a part of these effects. However no direct confrontation with the standard model has been achieved due to the lack of a consistent calculation of the long distance contributions to the weak matrix elements. However, we can now use the results of the previous section to make a consistent estimate of the full amplitudes including both short and long distance evolution effects.

The strict $1/N_C$ calculation gives an estimate of the nonfactorizing amplitudes of Figure 2. This amplitude can be separated into the usual two terms representing the short distance coefficient function and the nonfactorizing corrections to the weak matrix elements of the evolved weak operators. Because of the long evolution to the m_W scale, the renormalization group improvement can be systematically applied to the coefficient functions with a result which goes beyond the strict large N_C expansion. The prediction for the full amplitude combines these coefficient functions with the operator matrix elements.

We need the matrix element for both the Q_1 and Q_2 weak operators. There are about 100 Feynman diagrams for the three different matrix elements for $K \to \pi\pi$. The results of these calculations[1] are given by the amplitudes

$$\langle \pi^+\pi^- | Q_1(M^2) | K^0 \rangle = (X/f^2_\pi) \cdot F_1(M^2) \tag{23}$$

$$\langle \pi^+\pi^- | Q_2(M^2) | K^0 \rangle = X_F + (X/f^2_\pi) \cdot F_2(M^2) \tag{24}$$

$$\langle \pi^0\pi^0 | Q_1(M^2) | K^0 \rangle = - X_F - (X/f^2_\pi) \cdot F_3(M^2) \tag{25}$$

$$\langle \pi^0\pi^0 | Q_2(M^2) | K^0 \rangle = (X/f^2_\pi) \cdot [F_2(M^2) - F_1(M^2) - F_3(M^2)] \quad (26)$$

$$\langle \pi^+\pi^0 | Q_{1,2}(M^2) | K^+ \rangle \cdot \sqrt{2} = X_F + (X/f^2_\pi) \cdot [F_1(M^2) + F_3(M^2)] \quad (27)$$

where the factorized and leading order matrix elements, X_F and X, are

$$X_F = X \cdot [1 + (f_\pi/F_\pi) \cdot (F_K/F_\pi - 1) \cdot m^2_\pi/(m^2_K - m^2_\pi)] \quad (28)$$

$$X = \sqrt{2} \cdot F_\pi \cdot (m^2_K - m^2_\pi) \quad (29)$$

The cutoff dependent functions, $F_K(M^2)$, are computed from the nonfactorized meson loop amplitudes with the result

$$F_1(M^2) = (4\pi)^{-2} \cdot (f_\pi/F_\pi) \cdot [-2 \cdot M^2 + (m^2_K/4 + 19 \cdot m^2_\pi/9) \cdot \ln(1 + M^2/\tilde{m}^2)] \quad (30)$$

$$F_2(M^2) = (4\pi)^{-2} \cdot (f_\pi/F_\pi) \cdot [M^2 + (m^2_K - 3 \cdot m^2_\pi/2) \cdot \ln(1 + M^2/\tilde{m}^2)] \quad (31)$$

$$F_1(M^2) = (4\pi)^{-2} \cdot (f_\pi/F_\pi) \cdot [(8 \cdot m^2_\pi/9) \cdot \ln(1 + M^2/\tilde{m}^2)] \quad (32)$$

where $\tilde{m}$ is a common infrared scale, $m_\pi < \tilde{m} < m_K$, introduced for simplicity. Note that the quadratic divergences are precisely those given in Eqs.(19,20,21) as calculated from the coset field calculation.

This calculation of the meson matrix elements can be combined with the previous calculation of the short distance evolution to obtain the prediction for the full physical amplitudes. The results are given in Table I as functions of the strange quark mass, m_s and the matching scale, $\mu = M$.

The results are sensitive to the value of the strange quark mass through the penguin matrix elements. The large $\Delta I = 1/2$ amplitudes are rather insensitive to the matching scale reflecting the cancellation between the operator matrix elements and the short distance coefficient functions. The various contributions for the $K^0 \to \pi^+\pi^-$ decay amplitudes are given as functions of the matching scale in Table II.

Table I: Weak Decay Amplitudes

m_s(MeV)	μ=M(GeV)	$K^0\to\pi^+\pi^-$	$K^0\to\pi^0\pi^0$	$K^+\to\pi^+\pi^0$
	0.6	22.9	20.3	1.75
125	0.7	22.3	20.0	1.58
	0.8	22.2	20.3	1.33
	0.6	20.4	17.9	1.75
150	0.7	20.1	17.8	1.58
	0.8	20.1	18.2	1.33
	0.6	19.0	16.5	1.75
175	0.7	18.8	16.5	1.58
	0.8	18.8	17.0	1.33
Data		27.7	26.3	1.84

Table II: Separate Contributions

μ=M(GeV)	SD(Q_1,Q_2)	LD(Q_1,Q_2)	Penguin	Sum
0.6	9.3	5.6	5.5	20.4
0.7	8.7	6.4	5.1	20.2
0.8	8.3	7.0	4.8	20.1

The long distance contributions continue the normal weak mixing of the Q_1, Q_2 operators as well as additions to the penguin. With these matching scales, there are approximately equal contributions to the $\Delta I=1/2$ amplitudes from the short distance, long distance and penguins terms.

The calculation achieves about 3/4 of the actual enhancement of the $\Delta I=1/2$ amplitudes with significant strength in the long distance component. It also achieves about the right suppression of the $\Delta I=3/2$ amplitudes with about 1/3 of the total suppression due to long distance effects. This estimate of the strong interaction effects seems fully capable of explaining the K-meson decay amplitudes. The remaining discrepancy for the $\Delta I=1/2$ amplitudes may be resolved by improving our crude estimates of the meson and quark contributions to the nonfactorized diagrams of Figure 2. However, it may also require higher order $1/N_C$ corrections which are difficult to estimate without a

better separation of the short and long distance contributions to the amplitudes; here a practical formulation of the hadron string theory would be helpful.

6.2. Weak Mixing, the B_K Parameter

Weak mixing occurs due to the incomplete GIM cancellation for the $\Delta S=2$ processes which lead to $K^0 \rightleftarrows \overline{K^0}$ transitions. The basic box diagrams for these transitions are dominated by short distance processes. Standard renormalization group methods[5] can be applied to integrate out the short distance physics in favor of an effective four fermion operator, $Q = (\overline{S}\, D)_L \cdot (\overline{S}\, D)_L$. The transition amplitude is given by

$$\langle \overline{K^0} \,|\, H_{WK} \,|\, K^0 \rangle = \{ \eta_1(\mu) \cdot m_c^2 + \eta_2(\mu) \cdot m_t^2 + \eta_3(\mu) \cdot m_c^2 \cdot \log(m_t^2/m_c^2) \} \cdot \langle \overline{K^0} \,|\, Q(\mu) \,|\, K^0 \rangle \tag{33}$$

The coefficient functions evolve with anomalous dimensions associated with the four fermion operator which transforms as the $\underline{27}$ representation of SU(3). The same class of diagrams given in Figures 1,2 applies to this process and a similar separation of the weak matrix elements can be made as in the previous section. The B_K parameter is defined as

$$\langle \overline{K^0} \,|\, Q(\mu) \,|\, K^0 \rangle = B_K(\mu) \cdot (16/3) \cdot F_K^2 \cdot m_K^2 \tag{34}$$

Using full factorization, including Fierz terms, $B_K = 1$. In the leading order of the large N_C expansion, $B_K = 3/4$ because the Fierz terms are dropped. The factorizing contributions generate the renormalized, physical value of F_K in Eq.(34). The long distance, nonfactorizing contributions can be calculated from the meson loops.

$$\langle \overline{K^0} \,|\, Q(\mu) \,|\, K^0 \rangle_{meson} = 4 \cdot F_K^2 \cdot m_K^2 \cdot \{ -(4\pi \cdot F_K)^{-2} \cdot [2 \cdot M^2 - (10/3) \cdot m_K^2 \cdot \log(1 + M^2/\tilde{m}^2)\,] \} \tag{35}$$

Combining this result with the factorized amplitude, the B_K parameter becomes

$$B_K(M) = (3/4)\cdot\{1 - (4\pi\cdot F_K)^{-2}\cdot[2\cdot M^2 - (10/3)\cdot m^2_K\cdot\log(1+M^2/\tilde{m}^2)\,]\,\} \tag{36}$$

which must be adjusted to the usual definition of the B_K parameter by the appropriate short distance evolution. By varying the precise matching conditions[9], this estimate gives

$$B_K = 0.7 \pm 0.1 \tag{37}$$

It is interesting to compare the matrix elements for K^0-$\overline{K^0}$ mixing and $\Delta I=3/2$ K-meson decays. These transitions involve different matrix elements of four fermion operators in the same SU(3) representation,

$$\langle\overline{K^0}\,|\,Q(\mu)\,|\,K^0\rangle = 4\cdot F^2_K\cdot m^2_K\cdot\{\,1 - (4\pi\cdot F_K)^{-2}\cdot[2\cdot M^2 - (10/3)\cdot m^2_K\cdot\log(1+M^2/\tilde{m}^2)\,]\,\} \tag{38}$$

and

$$\langle\pi^+\pi^0\,|\,Q_2(\mu)\,|\,K^+\rangle = F_K\cdot(m^2_K - m^2_\pi)\cdot\{\,1 - (4\pi\cdot F_K)^{-2}\cdot[2\cdot M^2 - ((1/4)\cdot m^2_K + 3\cdot m^2_\pi)\cdot\log(1+M^2/\tilde{m}^2)\,]\,\} \tag{39}$$

The quadratic divergences are identical, reflecting the common anomalous dimension. The coefficient of the log divergences differ, reflecting the explicit chiral symmetry breaking. For a matching scale, $M \approx \mu \approx 700$ MeV, the long distance corrections for K^0-$\overline{K^0}$ mixing are small as the quadratic term is cancelled by large log terms in Eq.(38). For the K-meson decay matrix element, the log terms are small and the quadratic term provides the additional suppression needed to explain the observed magnitude of the $\Delta I=3/2$ amplitude.

6.3. CP Violating Amplitudes, ε'/ε

The direct CP violating amplitudes come from "top" penguin contributions. The methods described above can be used to calculate ε'/ε. The result depends on the KM angles as well as the value of the top quark mass. Under some assumptions[10], the predicted values are

$$\varepsilon'/\varepsilon = (3.2 \to 1.1)\cdot 10^{-3}, \quad m_t = (40 \to 100)\ \text{GeV} \tag{40}$$

7. CONCLUSIONS - OUTLOOK

The large N_C expansion permits a consistent calculation of both short and long distance contributions to the nonleptonic weak matrix elements. The calculations imply that there is significant strength contained in the long distance physics. For the K-meson decay amplitudes, about 3/4 of the observed enhancement of the physical $\Delta I=1/2$ amplitudes is identified while the full suppression of the $\Delta I=3/2$ amplitude is achieved, as shown in Tables I,II. The B_K parameter is computed to be $B_K = 0.7 \pm 0.1$. The CP violating decay amplitudes imply that $\varepsilon'/\varepsilon = (1.1 \rightarrow 3.2) \cdot 10^{-3}$.

This analysis represents the first attempt at consistent calculation of the weak matrix elements in the continuum field theory. The explicit calculations can clearly be greatly improved. The short distance, quark-gluon theory could be taken to higher order in perturbative QCD and certain nonperturbative aspects, such as dynamical symmetry breaking, could be included. The long distance, truncated meson theory could include higher derivative interactions or higher mass meson resonances. A more precise procedure for matching the long and short distance component could also be achieved. Higher order terms in the large N_C expansion appear difficult to include in this formalism without something like a practical hadronic string theory. There is also no direct extension of these techniques to heavy quark systems as it is more difficult to separate the effects of the short and long distance components.

It is encouraging that even the simplest approximations seem to yield consistent results in good agreement with the observed phenomenolgy. These results should be compared with those of lattice gauge theory which provides an alternative consistent method for calculating these processes, not restricted by the limitations of the large N_C expansion.

ACKNOWLEDGEMENTS

This research was done in collaboration with A.J. Buras and J.-M. Gerard. I wish to thank the Max-Planck-Institute for its hospitality and support of the Ringberg Workshop.

REFERENCES

1] W.A. Bardeen, A.J. Buras and J.-M. Gerard, Phys. Lett. **180B** (1986) 133; **192B** (1987) 138; Nucl. Phys. **B293** (1987) 787.

2] G. 't Hooft, Nucl. Phys. **B72** (1974) 461; E. Witten, Nucl. Phys. **B160** (1979) 57; S. Coleman, Erice Lectures (1979).

3] S.G. Callan, N. Coote, D.J. Gross, Phys. Rev. **D13** (1976) 1649; M.B. Einhorn, Phys. Rev. **D14** (1976) 3451; R. Brower, J. Ellis, M. Schmidt and J. Weis, Nucl. Phys. **B128** (1977) 131,175.

4] M.K. Gaillard, B.W. Lee, and J.L. Rosner, Rev. Mod. Phys. **47** (1975) 277; N. Cabbibo and L. Maiani, Phys. Lett. **73B** (1978) 418; D. Fakirov and B. Stech, Nucl. Phys. **B133** (1978) 315.

5] M.K. Gaillard and B.W. Lee, Phys. Rev. Lett. **33** (1974) 351; G. Altarelli and L. Maiani, Phys. Lett. **52B** (1974); F.J. Gilman and M.B. Wise, Phys. Rev. **D20** (1979) 2392.

6] C. Lovelace, Phys. Lett. **28B** (1968) 264.

7] J. Gasser and H. Leutwyler, Phys. Rep. **87C** (1982) 77; C. Bernard et al, Phys. Rev. **D32** (1985) 2343; R.J. Crewther, Nucl. Phys. **B264** (1986) 277; R.S. Chivukula, J.M. Flynn and H. Georgi, Phys. Lett. **171B** (1986) 453.

8] J. Bijnens, Phys. Lett. **152B** (1985) 226; J. Bijnens and B. Guberina, Phys. Lett. **205B** (1988) 103; J.L. Goity, Bern Preprint 1988.

9] F.J. Gilman and M.B. Wise, Phys. Rev. **D27** (1983) 1128; J. Bijnens, H. Sonoda, and M.B. Wise, Phys Rev. Lett. **53** (1984) 2367; W.A. Bardeen, A.J. Buras and J.-M. Gerard, Phys. Lett. (1988).

10] A.J. Buras and J.-M. Gerard, Phys. Lett. **203B** (1988) 272.